

# Supporting Information

## Post Synthetically Modified IRMOF-3 for Efficient Recovery and Selective Sensing of Uranium (VI) from Aqueous Medium

*V. Venkata Sravani<sup>1,2</sup>, Sarita Tripathi<sup>1,2</sup>, B. Sreenivasulu<sup>2</sup>, Satendra Kumar<sup>2</sup>, S. Maji<sup>2</sup>, C. V. S. Brahmmananda Rao<sup>1,2</sup>, A. Suresh<sup>\*1,2</sup>, and N. Sivaraman<sup>1,2</sup>*

<sup>1</sup>Homi Bhabha National Institute, Indira Gandhi Centre for Atomic Research, Kalpakkam – 603 102, Tamil Nadu, India.

<sup>2</sup>Material Chemistry and Metal Fuel Cycle Group, Indira Gandhi Centre for Atomic Research, Kalpakkam – 603 102, Tamil Nadu, India.

---

Corresponding author:

Dr. A. Suresh,  
Head, Fuel Chemistry Division,  
Materials Chemistry and Metal Fuel Cycle Group,  
Indira Gandhi Centre for Atomic Research,  
Kalpakkam – 603102,  
Tamil Nadu, India.  
Tel. +91 44 27480500 – 24028  
Email:[asu@igcar.gov.in](mailto:asu@igcar.gov.in)

## **Table of Contents**

|   |         |
|---|---------|
| Table S1: Conversion of IRMOF-3 to varied functionalized MOFs                               | S3      |
| FTIR spectra of IRMOF-3 and PSM MOFs  | S4      |
| Powder XRD patterns for IRMOF-3 and PSM MOFs  | S4      |
| TGA plot of IRMOF-3 and PSM MOFs  | S5      |
| 100.61 MHz $^{13}\text{C}$ -NMR spectra (DMSO- $d_6$ ) of PSM MOFs                          | S5      |
| $^{31}\text{P}$ NMR spectra (161.92 MHz, $^1\text{H}$ decoupled)of IRMOF-DPC in DMSO- $d_6$ | S6      |
| SEM and EDX spectra of IRMOF-3 and PSM MOFs   | S6-S9   |
| Table S2: BET surface area of IRMOF-3 and PSM MOFs  | S10     |
| Effect of contact time on uranium (VI) sorption onto MOFs                                   | S11     |
| Kinetic study   | S12-S13 |
| Table S3: Kinetic parameters for uranyl ion sorption on the MOFs                            | S13     |
| Desorption studies  | S14     |
| Sensing studies of uranium(VI) with competing metal ions using IRMOF-3<br>and PSM MOFs      | S15-S16 |
| Table S4: Langmuir model fitting of uranium (VI) fluorescent sensing studies<br>using MOFs  | S17     |

**Table S1.** Conversion of IRMOF-3 to different functionalized MOFs

| MOF       | % Conversion |
|-----------|--------------|
| IRMOF-PC  | 62%          |
| IRMOF-GA  | 70%          |
| IRMOF-SMA | 68%          |
| IRMOF-DPC | 72%          |

The percentage conversion of the amine groups in the IRMOF-3 to varied functionalized MOFs was determined by comparing the relative integrated areas of the aromatic resonances (corresponding to the C-3 position of the BDC ring) between the modified and unmodified BDC ligands.

1. Luan, Y., Zheng, N., Qi, Y., Tang, J. & Wang, G. Merging metal-organic framework catalysis with organocatalysis: A thiourea functionalized heterogeneous catalyst at the nanoscale. *Catal. Sci. Technol.* **2014**, 4, 925-929.

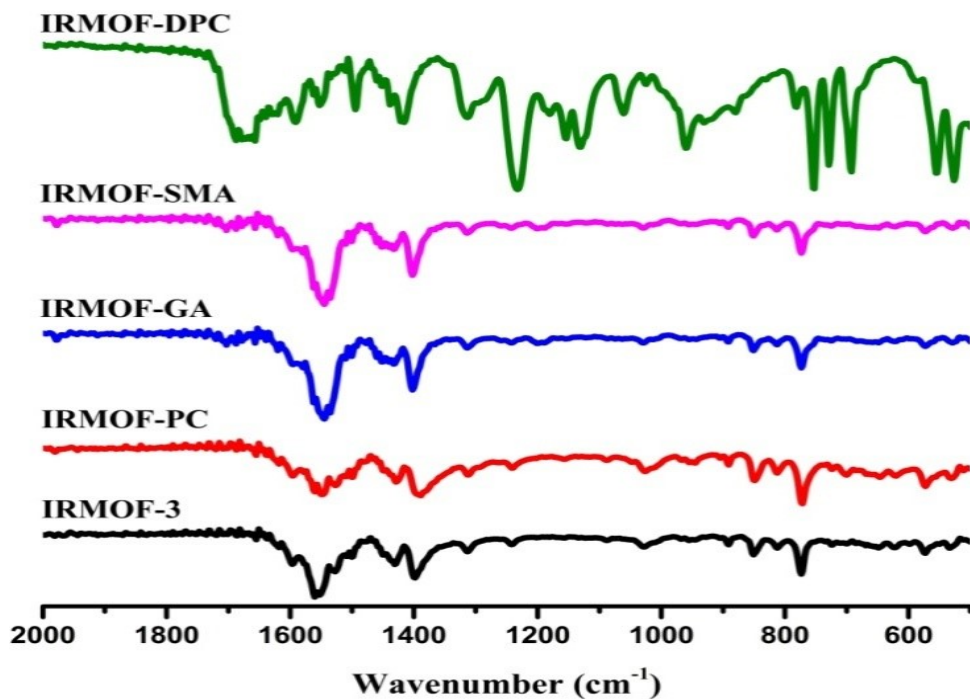


**Figure S1.** FTIR spectrum of IRMOF-3 and its functionalized MOFs.

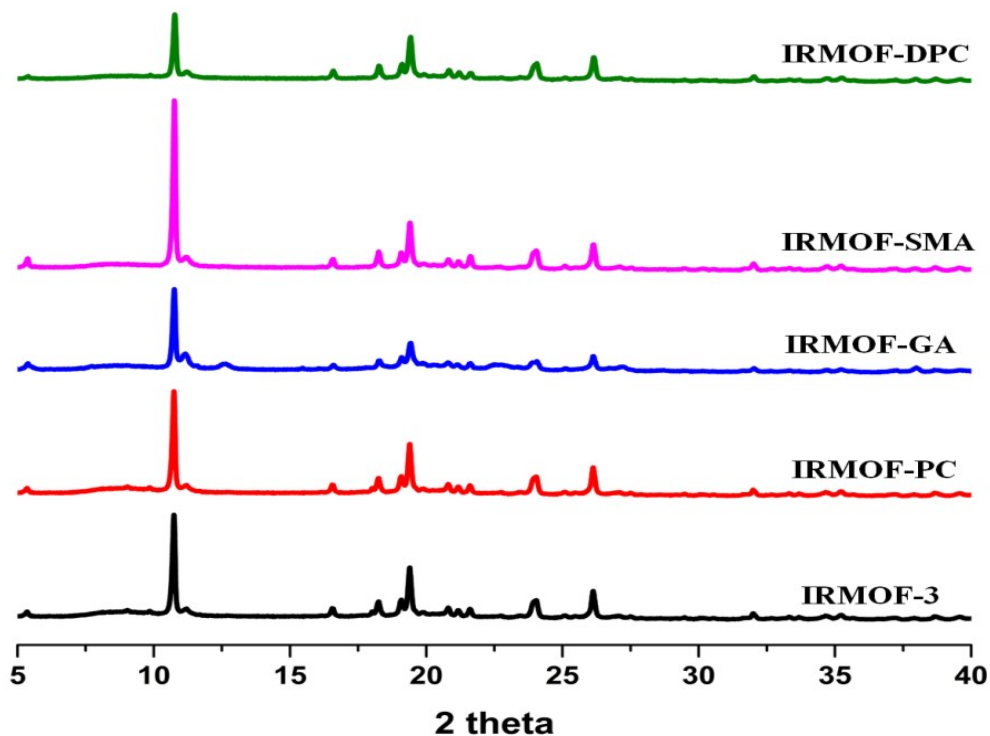


**Figure S2.** Powder XRD patterns of IRMOF-3 and its functionalized MOFs.

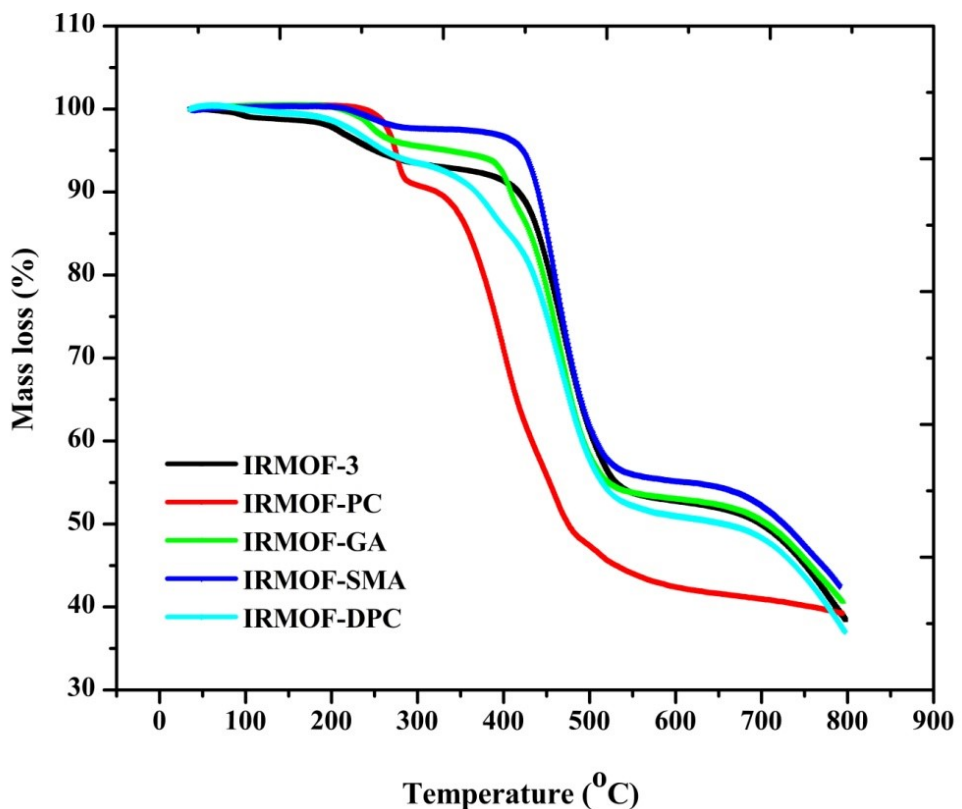


**Figure S3.** TGA plot of IRMOF-3 and its functionalized MOFs.

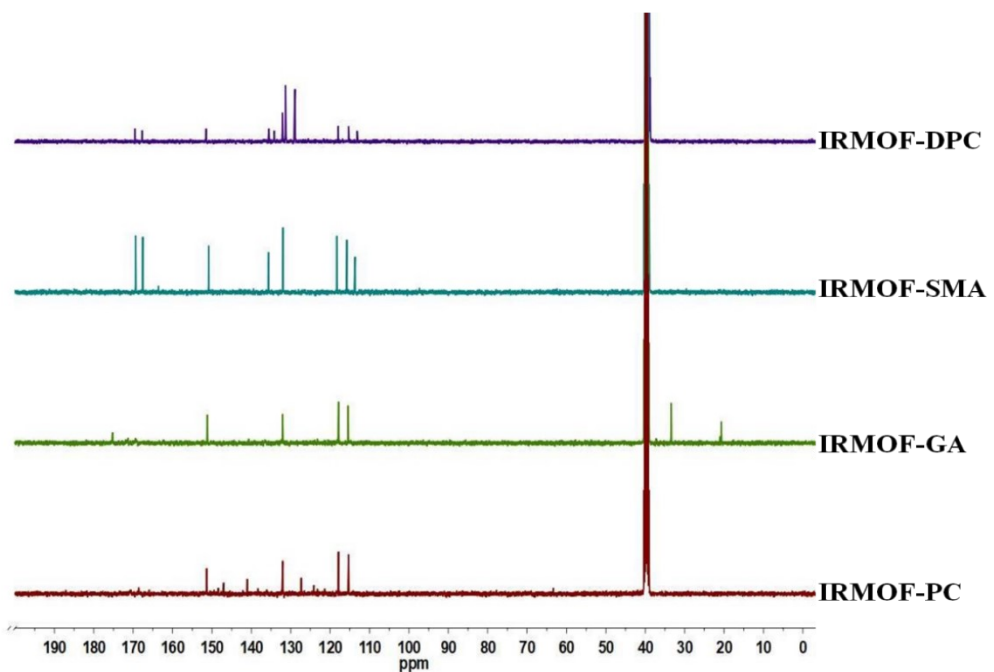


**Figure S4.** <sup>13</sup>C-NMR (100 MHz, in DMSO-*d*<sub>6</sub>) spectra of PSM MOFs.

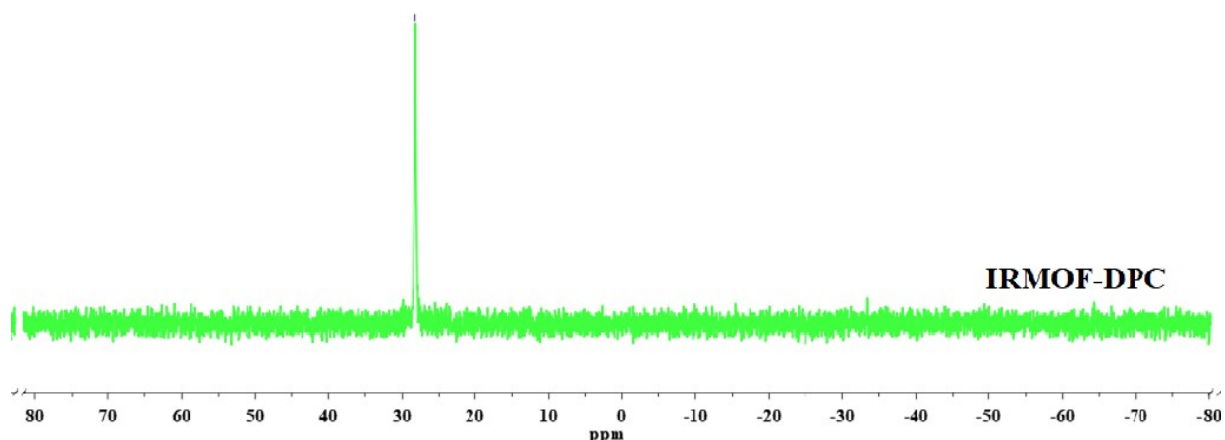


**Figure S5.**  $^{31}\text{P}$ -NMR (162MHz,  $^1\text{H}$  decoupled) in  $\text{DMSO}-d_6$  of IRMOF-DPC.

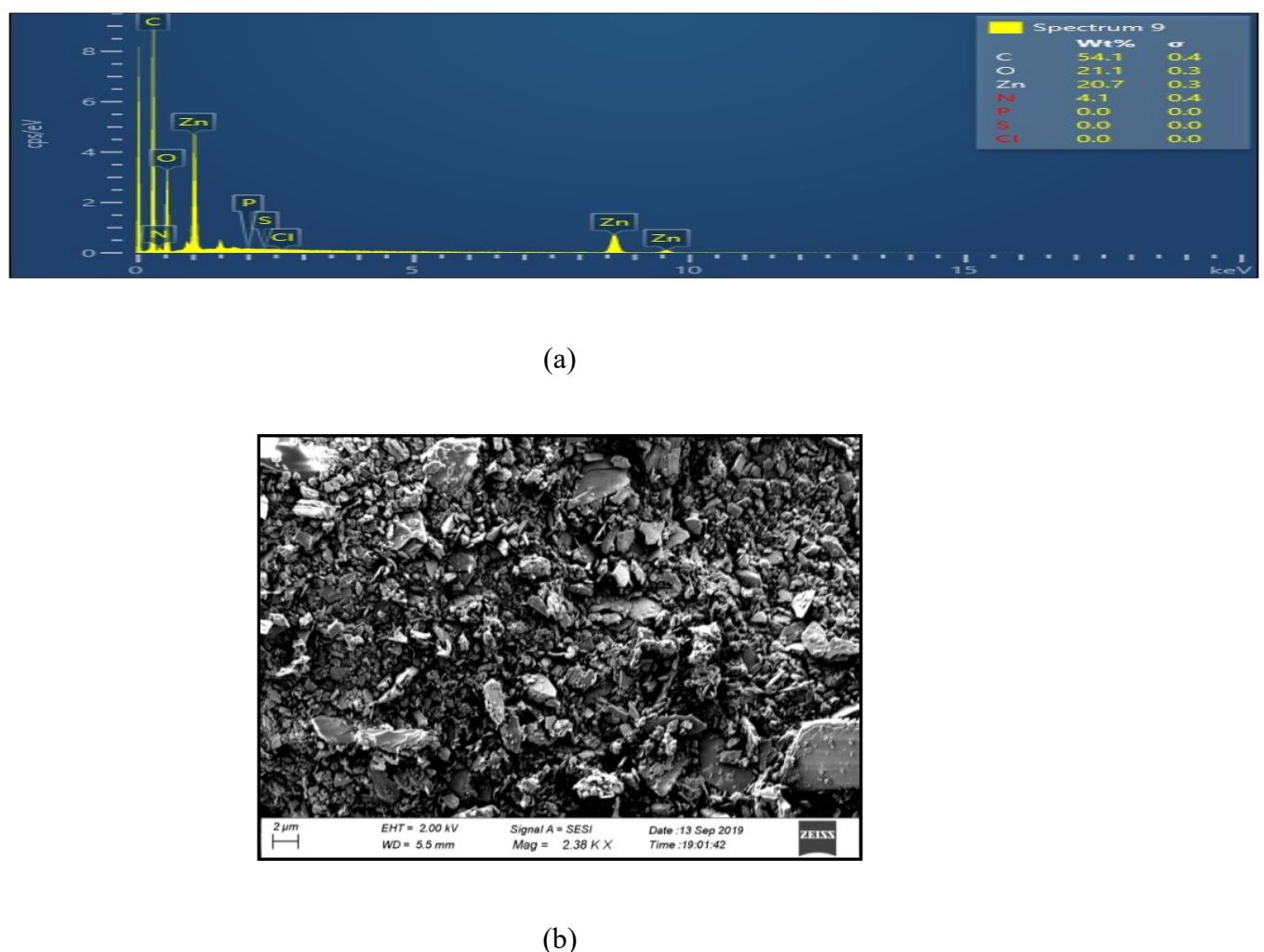


**Figure S6.** (a) EDX spectra and (b) SEM image of IRMOF-3.

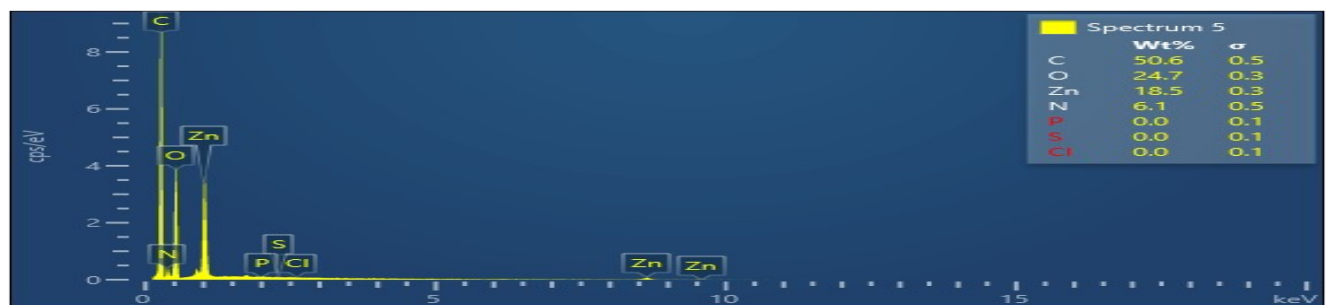


(a)

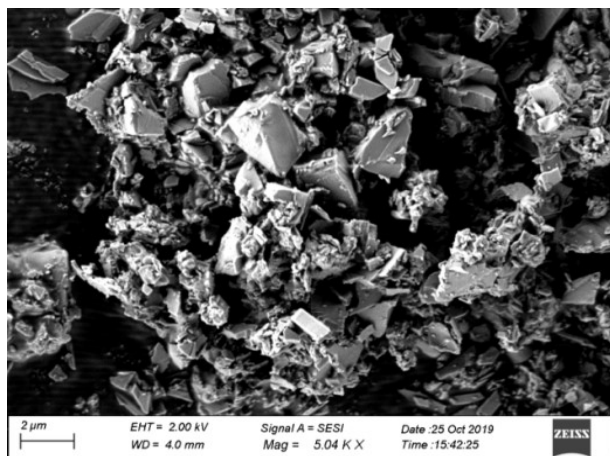


(b)

**Figure S7.** (a) EDX spectra and (b) SEM image of IRMOF-PC.

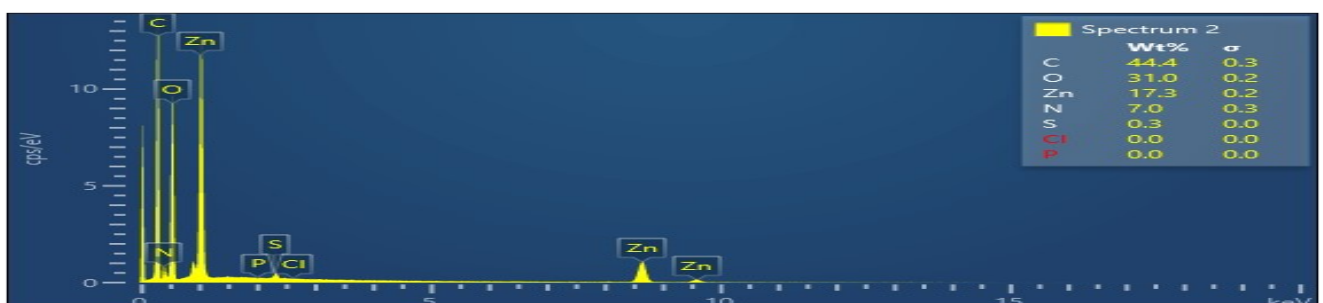


(a)

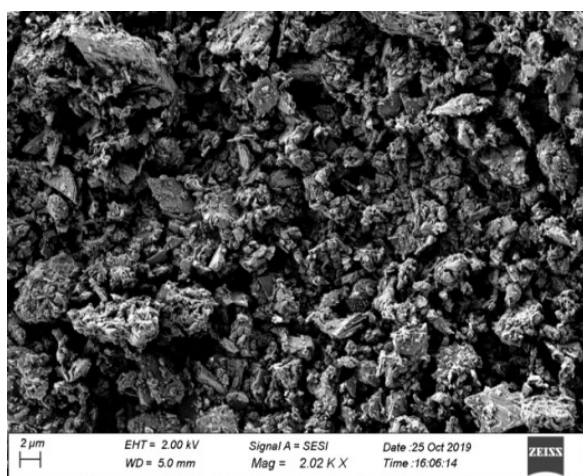


(b)

**Figure S8.** (a) EDX spectra and (b) SEM image of IRMOF-GA.

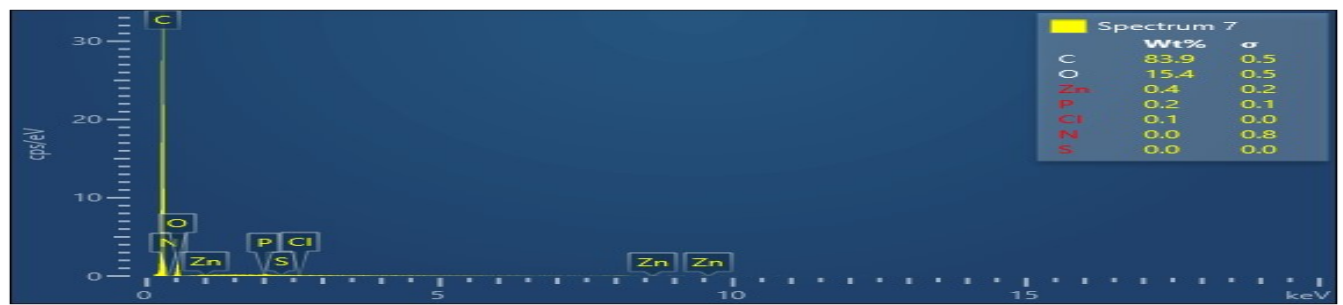


(a)

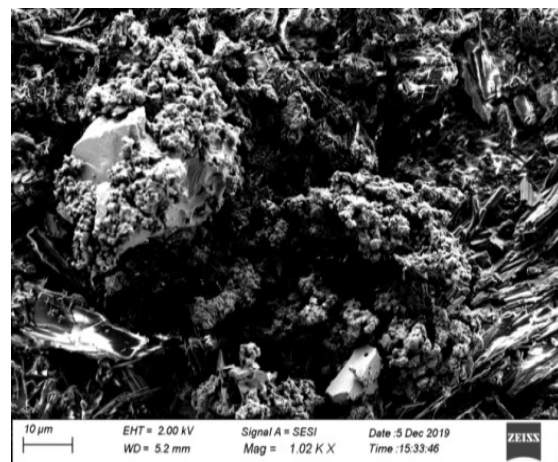


(b)

**Figure S9.** (a) EDX spectra and (b) SEM image of IRMOF- SMA.



(a)



(b)

**Figure S10.** (a) EDX spectra and (b) SEM image of IRMOF-DPC.

**Table S2.** BET surface area of IRMOF-3 and different functionalized MOFs

| MOF       | BET Surface area ( $\text{m}^2\text{g}^{-1}$ ) |
|-----------|--|
| IRMOF-3   | 2440 <sup>1</sup>                              |
| IRMOF-PC  | 1988   |
| IRMOF-GA  | 1870   |
| IRMOF-SMA | 2052   |
| IRMOF-DPC | 1910   |

1. Gascon, J., Aktay, U., Hernandez-Alonso, M. D., van Klink, G. P. M. & Kapteijn, F. Amino-based metal organic frameworks as stable, highly active basic catalysts. *J. Catal.* **2009**, 261, 75-87.

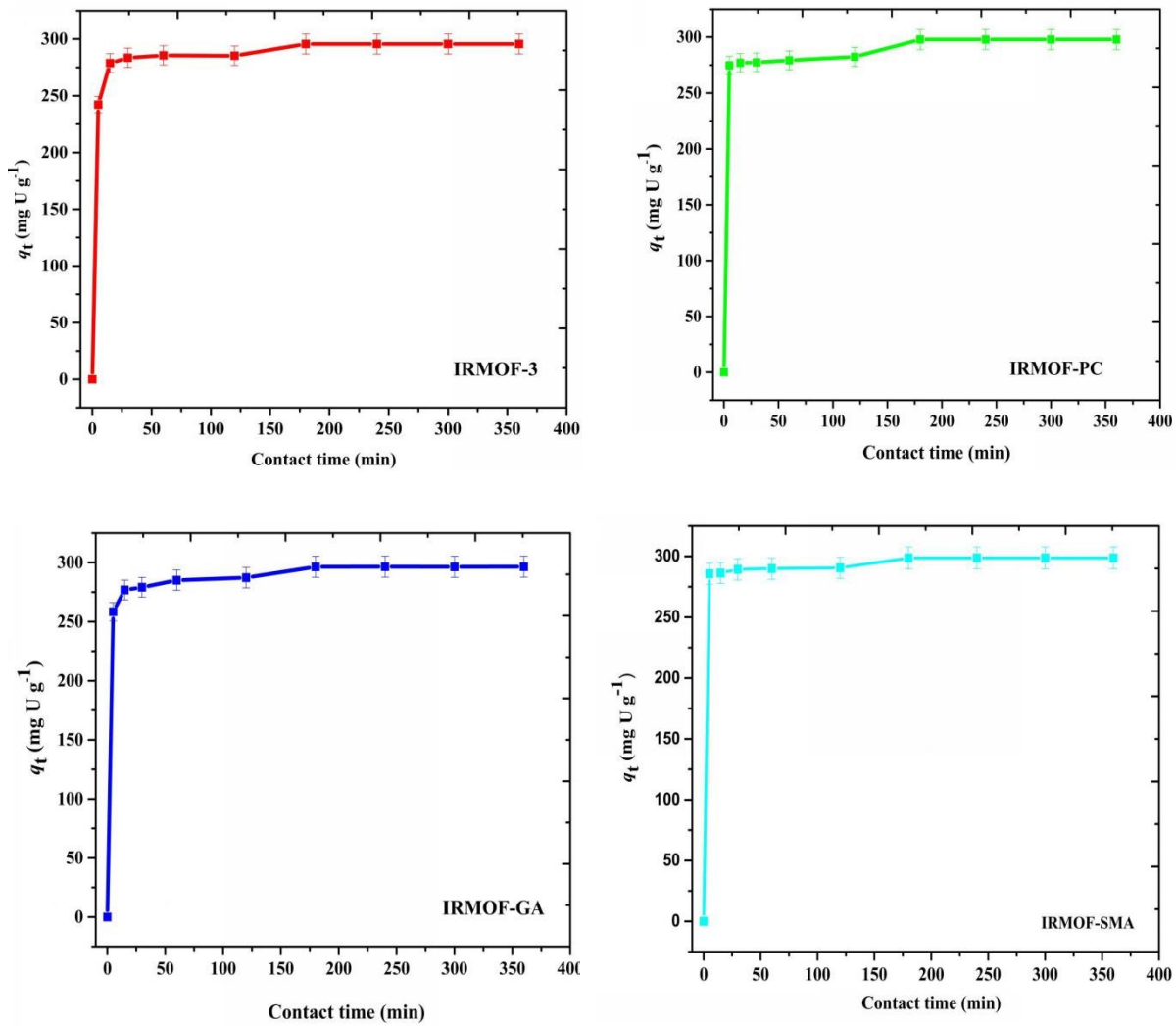


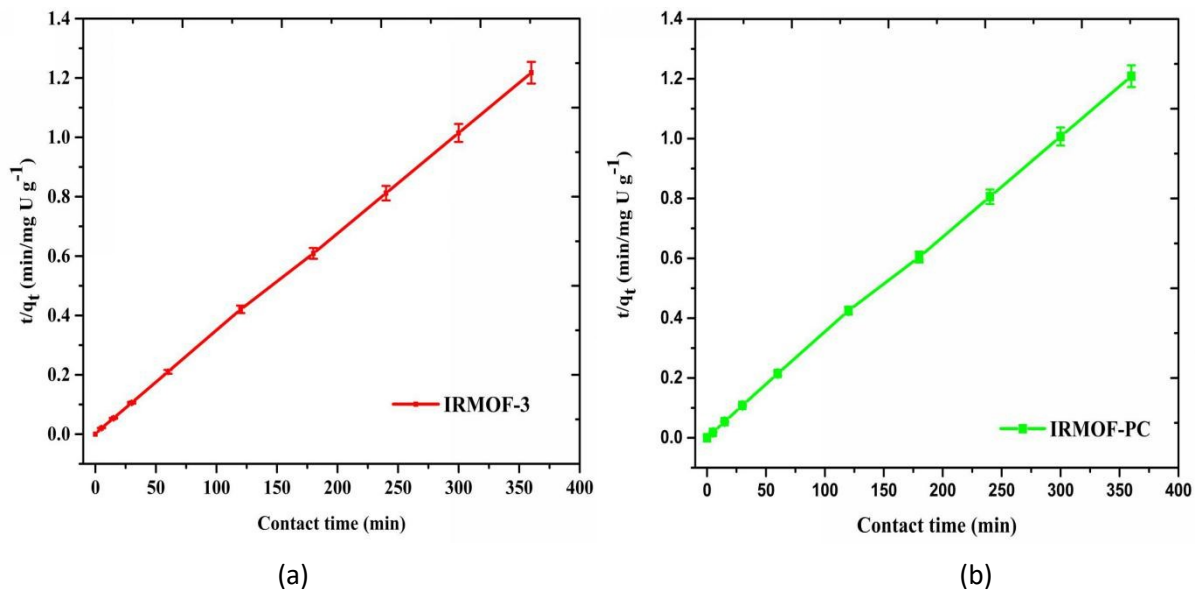
**Figure S11.** Effect of contact time on uranium (VI) sorption (%) onto (a) IRMOF-3, (b) IRMOF-PC, (c) IRMOF-GA, (d) IRMOF-SMA; pH = 6,  $m_{\text{sorbent}} = 10.0$  mg,  $V_{\text{solution}} = 3$  mL,  $C_0 = 1$  mg/mL,  $T = 25 \pm 1^\circ\text{C}$ .

## Kinetic model

The plot of  $t/q_t$  vs  $t$  for IRMOF-3 and its PSM MOFs given the straight line and the linear form of the pseudo-second-order kinetic model is expressed as follows:

$$\frac{t}{q_t} = \frac{1}{K_2 q_e^2} + \frac{t}{q_e}$$

Where  $q_e$  ( $\text{mg}\cdot\text{g}^{-1}$ ) and  $q_t$  ( $\text{mg}\cdot\text{g}^{-1}$ ) are the amounts of the uranium absorption at equilibrium and at time  $t$ , respectively. And  $K_2$  ( $\text{g}\cdot\text{mg}^{-1}\cdot\text{min}^{-1}$ ) is the pseudo-second-order sorption rate constant. The model parameters and the correlation coefficient obtained are shown in Table S3.



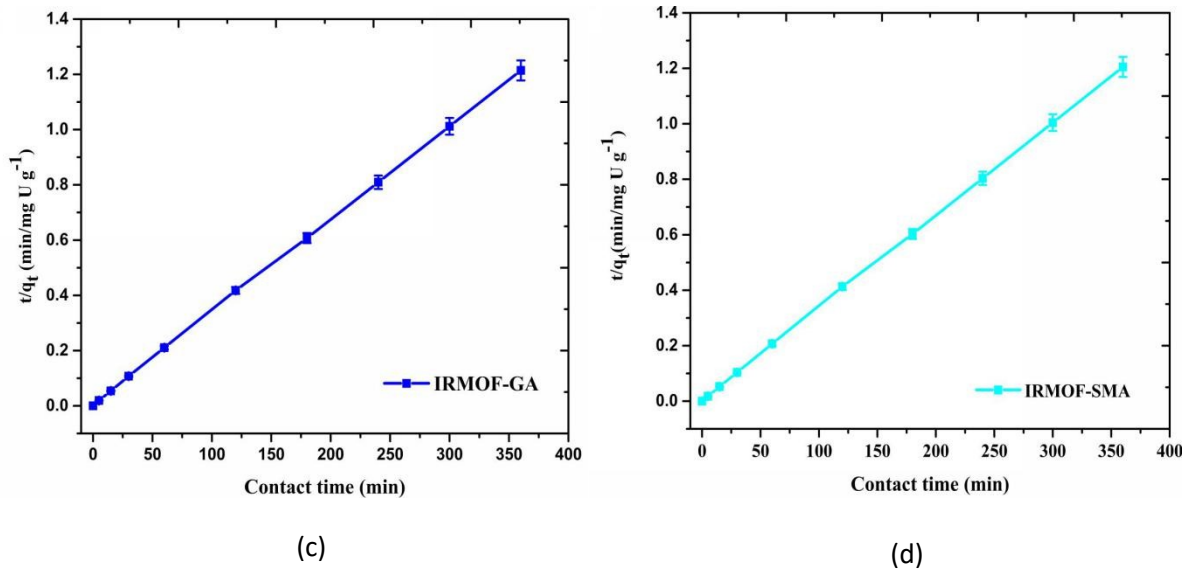


**Figure S12:** Pseudo-second-order model fits for the kinetic rate on the sorbent (a) IRMOF-3, (b) IRMOF-PC, (c) IRMOF-GA, (d) IRMOF-SMA.

**Table S3.** Kinetic parameters for uranium (VI) sorption on the MOFs

| Pseudo-second-order kinetic model |                             |  |                |
|-----------------------------------|-----------------------------|--|----------------|
| MOF                               | $q_e$ (mg·g <sup>-1</sup> ) | $K_2$ (g·mg <sup>-1</sup> ·min <sup>-1</sup> ) | R <sup>2</sup> |
| <b>IRMOF-3</b>                    | 270 ± 8                     | 0.00489  | 0.9998         |
| <b>IRMOF-PC</b>                   | 285 ± 8                     | 0.00694  | 0.9997         |
| <b>IRMOF-GA</b>                   | 280 ± 8                     | 0.0051   | 0.9999         |
| <b>IRMOF-SMA</b>                  | 290 ± 8                     | 0.00339  | 0.9999         |
| <b>IRMOF-DPC</b>                  | 299 ± 8                     | 0.00109  | 0.9999         |

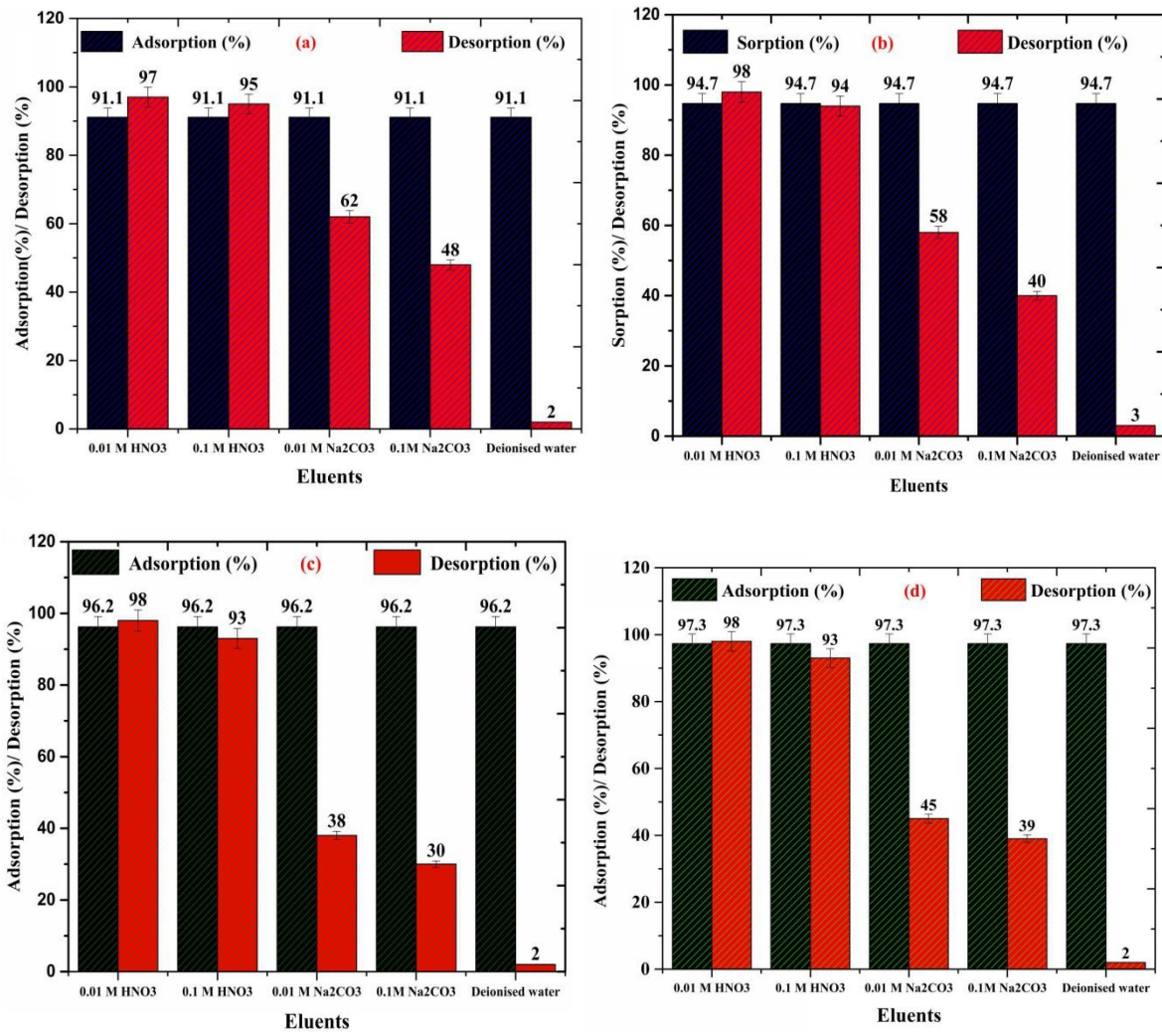


**Figure S13.** Sorption (%)/ Desorption (%) bar graphs of (a) IRMOF-3; (b) IRMOF-GA; (c) IRMOF-PC; (d) IRMOF-SMA with different eluents.

## Sensing studies of uranium (VI):

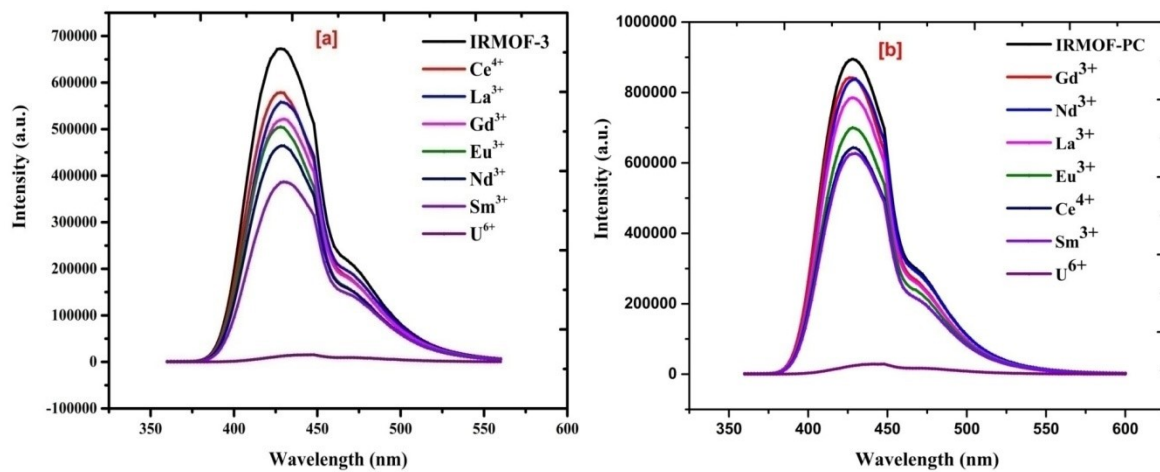
The detection limit for IRMOF-3 and its PSM MOFs was calculated as follows:

$$DT = \frac{3\sigma}{\text{Slope}}$$

$$\sigma = 100 \times \frac{I_{SE}}{I_0}$$

Here, DT is the detection limit,  $I_{SE}$  is the standard error of the luminescence intensity measurement, as determined by the baseline measurement of blank samples monitored at 428 nm, 426 nm, 330 nm, 424 nm, and 334 nm of IRMOF-3 and PSM MOFs(IRMOF-PC, IRMOF-GA, IRMOF-SMA, and IRMOF-DPC) respectively, and  $I_0$  is the measured luminescence intensity.

The slope was obtained from the linear fit of the uranyl concentration-dependent luminescence intensity curve in the 0-300 mg/L region (Figure 10 inset).



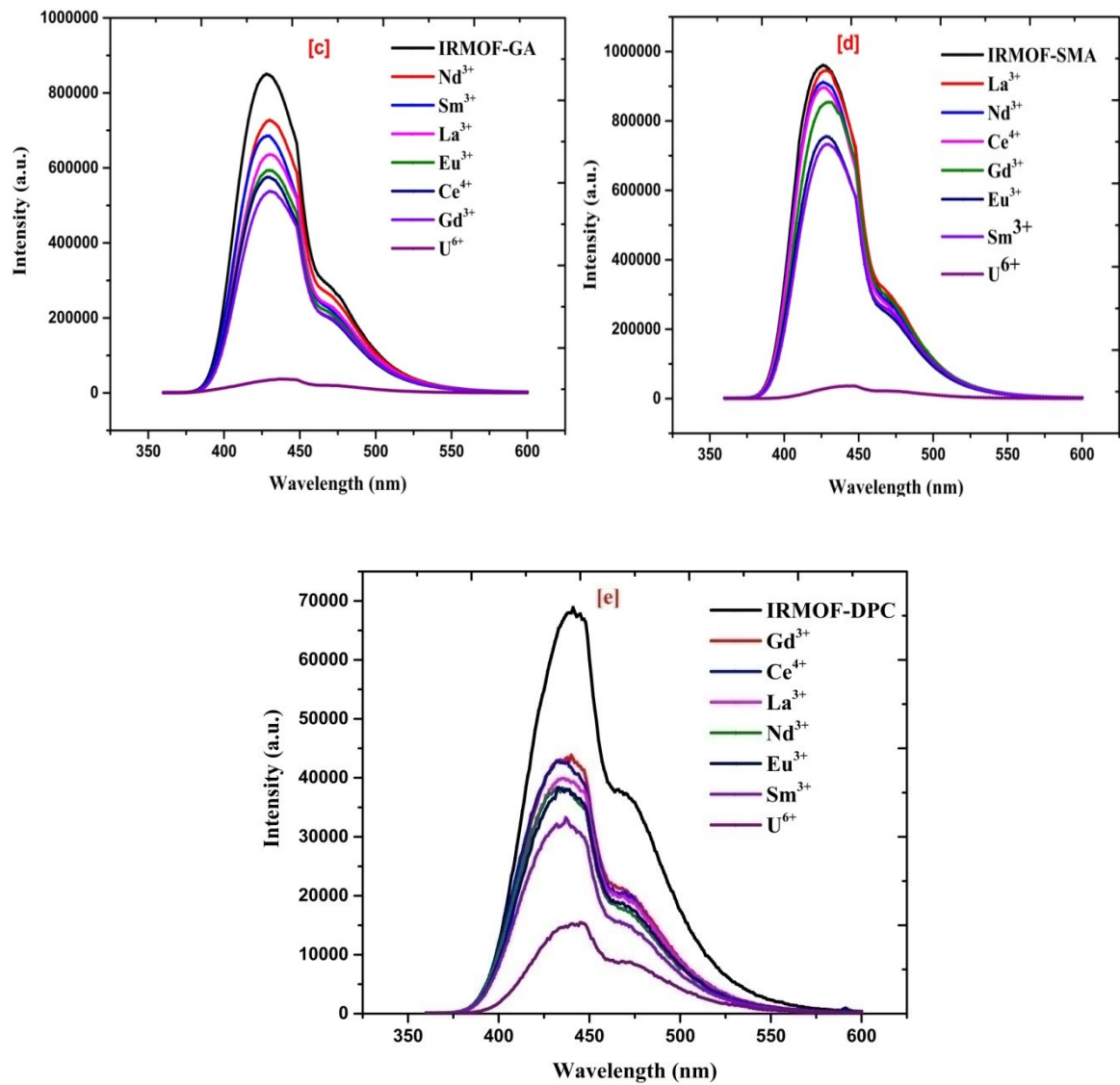


**Figure S14.** Emission spectra of (a) IRMOF-3, (b) IRMOF-PC, (c) IRMOF-GA, (d) IRMOF-SMA, and (e) IRMOF-DPC up on treatment of uranium (VI) and various competing metal ions ( $\text{La}^{3+}$ ,  $\text{Ce}^{4+}$ ,  $\text{Nd}^{3+}$ ,  $\text{Sm}^{3+}$ ,  $\text{Gd}^{3+}$ , and  $\text{Eu}^{3+}$ ) with standard concentration of 100 mg/L.

**Table S4:** The Langmuir model fitting of U(VI) fluorescent sensing using IRMOF-3 and its PSM MOFs

| S. No | MOF       | R <sup>2</sup> |
|-------|-----------|----------------|
| 1     | IRMOF-3   | 0.9988         |
| 2     | IRMOF-PC  | 0.9976         |
| 3     | IRMOF-GA  | 0.9993         |
| 4     | IRMOF-SMA | 0.9936         |
| 5     | IRMOF-DPC | 0.9986         |